JACS
JOURNAL OF THE AMERICAN CHEMICAL SOCIETY
Communication
pubs.acs.org/JACS

# Ammonia-Rich High-Temperature Superconducting Intercalates of Iron Selenide Revealed through Time-Resolved *in Situ* X-ray and Neutron Diffraction

Stefan J. Sedlmaier,[†] Simon J. Cassidy,[†,‡] Richard G. Morris,[†] Michael Drakopoulos,[‡] Christina Reinhard,[‡] Saul J. Moorhouse,[†,‡] Dermot O'Hare,[†] Pascal Manuel,[§] Dmitry Khalyavin,[§] and Simon J. Clarke*[,†]

[†]Department of Chemistry, Inorganic Chemistry Laboratory, University of Oxford, South Parks Road, Oxford OX1 3QR, United Kingdom

[‡]Diamond Light Source Ltd., Harwell Science and Innovation Campus, Didcot OX11 0DE, United Kingdom

[§]ISIS Facility, STFC Rutherford Appleton Laboratory, Harwell Oxford, Didcot OX11 0QX, United Kingdom

Supporting Information

**ABSTRACT:** The development of a technique for following *in situ* the reactions of solids with alkali metal/ammonia solutions, using time-resolved X-ray diffraction methods, reveals high-temperature superconducting ammonia-rich intercalates of iron selenide which reversibly absorb and desorb ammonia around ambient temperatures.

Iron-based superconductors exhibit rich chemistry and physics. Control of the transition between itinerant antiferromagnetism and superconductivity in several iron arsenides, selenides, and phosphides is possible using applied pressures and isovalent or aliovalent substitutions to tune structural parameters and/or electron count. Understanding these materials' superconducting and magnetic properties may shed light on the behavior of other classes of high-temperature superconductor. Recent reviews describe developments in synthesis,[1] structure−property relationships,[2] materials properties,[3] and theory.[4]

The tetragonal layered polymorph of FeSe is a superconductor[5] with a superconducting transition temperature ($T_c$) of 8.5 K for the composition $Fe_{1.01}Se$ (a small amount of intrinsic interstitial iron has a detrimental effect on superconductivity).[6] Ying et al.[7] revealed that solutions of alkali metals in liquid ammonia react with FeSe to produce intercalates with dramatically enhanced $T_c$'s of up to 45 K. We showed,[8] in the case of the intercalates obtained from Li/$ND_3$ solutions, that the crystal structures of the products obtained after evaporation of the ammonia solvent and brief evacuation of the reaction vessels at room temperature are variants of the common $ThCr_2Si_2$ structure type, with $ND_3$ and $[ND_2]^-$ moieties in sites 8-coordinated by selenide with N−D···Se hydrogen bonds. Li ions occupy sites coordinated by the ammonia or amide species and selenide (Figure 1, right). Scheidt et al. reported that amide-free materials may also be obtained.[9] The samples offer iron selenides with no iron vacancies and represent bulk variants of the minority phases which are presumed to be the source of superconductivity in $A_xFe_{2-y}Se_2$ samples ($x \approx 0.8$; $y \approx 1.6$; A = K, Rb, Cs) synthesized at high temperatures.[10,11] Ying et al.[12] report that ammonia may be completely removed from the intercalate

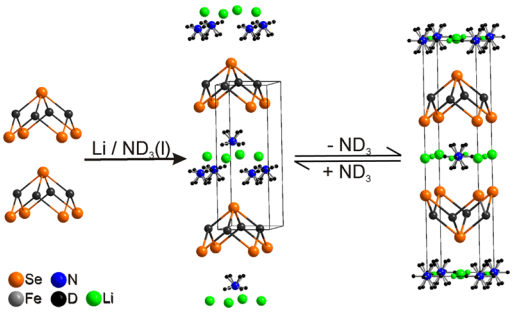


**Figure 1.** Schematic of the intercalation of lithium and ammonia into FeSe. The ammonia-rich intermediate is synthesized and described here; the structure and properties of the product of reversible ammonia desorption (right) is described in ref 8.

$K_{0.3}(NH_3)_{0.7}Fe_2Se_2$ ($T_c$ = 44 K) at 200 °C to yield a bulk superconducting phase $K_{0.3}Fe_2Se_2$ with the same $T_c$.

Here we describe a means to probe reactions using powder X-ray diffraction (PXRD) *in situ* in liquid ammonia at temperatures down to −78 °C and reveal that the metal/ammonia intercalates described previously[7−9,12] are the decomposition products obtained, in the normal course of handling solid-state compounds, from materials much richer in intercalated ammonia (Figure 1, center). The structure and properties of the ammonia-rich lithium/ammonia intercalate, and its reversible adsorption and desorption of ammonia, are described.

The syntheses of ammonia-rich FeSe intercalates were performed on the beamline, I12, at the Diamond Light Source, U.K. in an experiment conceived to investigate the intercalation *in situ* and identify possible intermediate phases. For the reactions between Li/$NH_3$ solutions and FeSe, 4 mg (0.576 mmol) of Li metal was loaded, in an argon-filled glovebox, into 18 mm o.d. × 4 mm wall Pyrex ampules sealed with Teflon valves. Synthesized from the elements as described previously,[8] 150 mg (1.113 mmol) of FeSe powder was loaded into a side arm projecting from the side of the ampule so that it was not in contact with the alkali metal (see the Supporting Information (SI)). The ampule was connected to a Schlenk line, the end of

**Received:** November 16, 2013
**Published:** December 19, 2013

   dx.doi.org/10.1021/ja411624q | J. Am. Chem. Soc. 2014, 136, 630−633

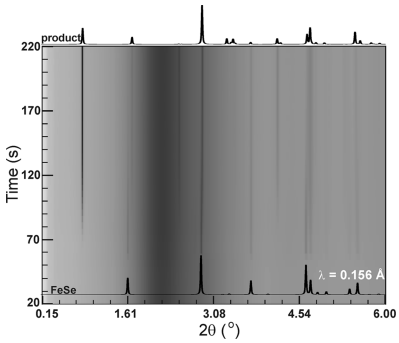


**Figure 2.** Film plot showing the evolution of the XRD pattern measured on I12 when FeSe was added to Li/$NH_3$ solution at ambient temperature. Calculated diffractograms are shown for FeSe and the final product. Further diffractograms (Figure S2) and a Rietveld analysis of the final product are shown in the SI.

the tube containing the alkali metal was placed in liquid nitrogen, and ∼5 $cm^3$ of $NH_3$ was condensed onto the alkali metal. On melting the $NH_3$ ice at −78 °C in a $CO_2$/propan-2-ol cooling bath, the alkali metal dissolved to produce a blue solution. The ampule was sealed and transported to the beamline keeping the solution separate from the solid FeSe. The ampules either were maintained with the end containing the solution in the $CO_2$/propan-2-ol slush or were allowed to warm to room temperature (for safety precautions see the SI). The ampule was clamped to a remote-controlled stage with its rotation axis parallel and coincident with the X-ray beam. With the stirred Li/$NH_3$ solution exposed to a monochromatic 80 keV ($\lambda$ = 0.156 Å) X-ray beam, diffractograms were measured continuously in time intervals of either 80 ms separated by a 40 ms dead time or 4 s separated by a 1 s dead time with data collected using a Thales Pixium RF4343 flat panel detector. To initiate the reaction, the ampule was rotated about the beam direction so that the FeSe powder poured into the solution. The evolution of the diffraction pattern was monitored over a period of a few minutes at ambient temperatures or a few hours at lower temperatures. This method is transferrable to other volatile solvent systems.

The *in situ* PXRD measurements of the reaction between Li/$NH_3$ solutions and FeSe initially showed the appearance of reflections due to FeSe. At ambient temperature (Figure 2) these reflections rapidly diminished in intensity to be replaced by a new set of reflections. These new reflections bore a superficial resemblance to those of the *I*4/*mmm* Li/$NH_3$ intercalates of FeSe reported previously[8] in which the lowest-angle Bragg peak is the (002) reflection with a *d*-spacing of ∼8.5 Å, corresponding to the separation between adjacent Fe planes. However the product of these reactions probed *in situ* had the lowest-angle Bragg peak at a *d*-spacing of 10.6 Å, 20% larger than in the intercalates described previously. After ∼2 min at ambient temperatures or 2.5 h at −78 °C, Bragg peaks due to FeSe had been completely replaced by those of the new material, which is the final product of these intercalation reactions when the solid remains suspended in liquid ammonia.

For these reactions $\alpha(t)$ for a particular Bragg reflection (*hkl*) is defined as the temporal evolution of $I(t)/I(\max)$ for that reflection. For a reaction with no intermediate phases the intensity evolution of reactant and product Bragg peaks should cross at $\alpha = 0.5$, while a crossing at $\alpha < 0.5$ suggests the presence of an intermediate phase.[13] In the case of the lithiation reaction shown in Figure 2 there appears to be a seamless transition between FeSe and the new product. However, plots of $\alpha(t)$ for the (001) Bragg reflections of FeSe and the product (Figure S10) cross at $\alpha \approx 0.4$ at room temperature, suggesting that an intermediate phase exists.

**Table 1. Lattice Parameters and Cell Volumes of the Final Products of Reactions of Alkali Metal/Ammonia Solutions with FeSe Determined from I12 PXRD Data (Figures S4−S6)**

| metal/FeSe ratio | *a* (Å) | *c* (Å) | *V* (Å$^3$) |
|---|---|---|---|
| Li/FeSe = 0.5 | 3.82766(8) | 10.5938(7) | 155.210(12) |
| K/FeSe = 0.15 | 3.8602(1) | 10.1793(1) | 151.7(12) |
| K/FeSe = 0.3 | 3.8348(5) | 9.8492(3) | 144.8(6) |
| Rb/FeSe = 0.5 | 3.8416(2) | 10.0408(7) | 148.2(19) |

The room-temperature diffractograms indeed revealed the presence of a crystalline intermediate phase (Figures S17 and S18), but the two observable reflections at *d*-spacings of 6.69 and 3.26 Å were insufficient to allow its identification. In low-temperature reactions, by contrast, the normalized intensities of FeSe and product (001) Bragg reflections cross at $\alpha \approx 0.1$ (Figures S12, S14, and S16), and film plots (Figures S11, S13, and S15) show a period between the near-disappearance of the FeSe reflections and the appearance of reflections from the product when little crystalline material is present.[13]

For the final product of Li/$NH_3$ intercalation, all reflections were indexed on a primitive tetragonal unit cell with refined room-temperature lattice parameters $a$ = 3.82766(8) Å and $c$ = 10.5938(7) Å. Systematic absences were consistent with the space groups *P*4/*n* or *P*4/*nmm*, and *ab initio* structure solution in *P*4/*nmm* using the charge-flipping algorithm as implemented in TOPAS Academic[14] resulted in a structural model with FeSe layers stacked as in the starting material FeSe (which also crystallizes in *P*4/*nmm*) but pushed apart, accommodating a double layer of light atoms (N atoms from the ammonia molecules) in the interlayer region. This is in contrast to the single layer of N atoms found in the case of the intercalates described previously.[8] This new model, with the PbFCl structure type (the "111" structure in the context of iron superconductors), gave an excellent Rietveld fit to the *in situ* PXRD data (Figure S3, Tables S1 and S2).

Similar reactions with solutions of K and Rb in $NH_3$ revealed similar general behavior: when PXRD measurements were performed *in situ*, phases were identified with much longer lattice parameters perpendicular to the FeSe layers (Table 1) than the ammonia-poor intercalates described previously.[7,12] The unit cell volumes for K/$NH_3$ intercalates decrease as the K content increases, which mirrors the observation by Ying et al. for the ammonia-poor K/$NH_3$ intercalates[12] and is presumably a consequence of an increased ionic bonding within the intercalate layers as the $K^+$ and amide content increases. The detailed crystal structures of the ammonia-poor and -rich K and Rb intercalates require further investigation.

To fully describe the structure of the new Li/ammonia intercalate, a 1 g sample of the ammonia-poor intercalate $Li_{0.6}(ND_3)_{0.8}(ND_2)_{0.2}Fe_2Se_2$ was placed in a thin-walled 8 mm diameter cylindrical vanadium container and attached to the Schlenk line. The sample container was evacuated briefly, then cooled to −10 °C by means of an ice/salt bath and then exposed to 1 atm of $ND_3$ gas (99% D). After 4 h the container was sealed, while cold, with a steel cap and an indium gasket under a stream of $ND_3$ gas. The mass change of the powder during loading suggested the absorption of ∼1 mol of $ND_3$ per mole of $Li_{0.6}(ND_3)_{0.8}(ND_2)_{0.2}Fe_2Se_2$. Powder neutron diffraction (PND) data collected at 270 K on WISH at the ISIS Facility, U.K.,


dx.doi.org/10.1021/ja411624q | J. Am. Chem. Soc. 2014, 136, 630−633

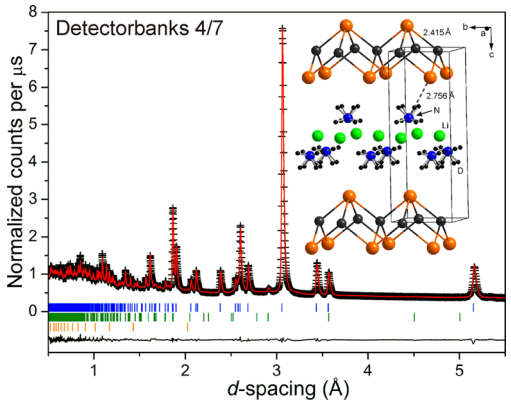


**Figure 3.** Observed (black crosses) and calculated (red line) PND pattern and difference profile of the Rietveld refinement of the structure of the deuterated ammonia-rich Li/$ND_3$ intercalate against WISH data at 5 K and the final crystal structure; peak positions are marked by vertical lines (intercalate, blue (99.4 wt%); $LiND_2$, green (0.2 wt%); Fe, orange (0.4 wt%).

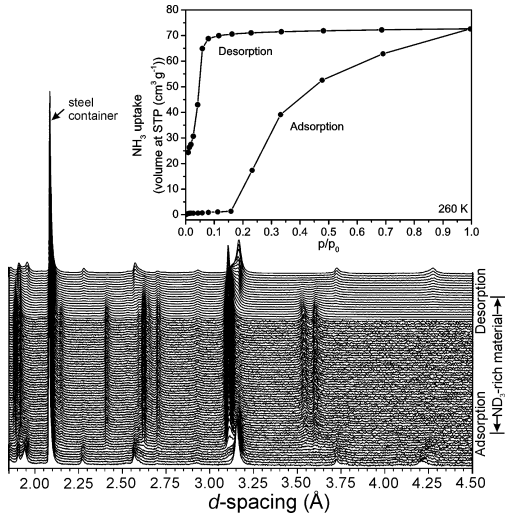


**Figure 4.** (Top) $NH_3$ adsorption and desorption isotherms for the ammonia-poor intercalate. (Bottom) PND patterns (WISH) during adsorption and desorption of $ND_3$ by the ammonia-poor intercalate at 250 K. The phases present are the $ND_3$-poor and -rich intercalates and the steel container.

revealed a diffraction pattern composed of a single phase consistent with the ammonia-rich intercalate obtained in the *in situ* XRD experiments (tetragonal P, $a$ = 3.81386(3) Å, $c$ = 10.5278(1) Å).

This confirms that compounds similar to those identified in the *in situ* PXRD measurements can be regenerated by exposure of the ammonia-poor intercalates[8] to ammonia at low temperatures. PND measurements on a second sample which had been exposed to 1 atm of $ND_3$ at 0 °C for 4 h revealed a mixture of just the new ammonia-rich and -poor[8] materials (see Figure S8), suggesting that absorption of further ammonia by the ammonia-poor material does not proceed via any other stable phase. A longer PND data collection at 5 K on the pure $ND_3$-rich intercalate (Figure 3) confirmed the partial structure derived from the *in situ* XRD experiments and enabled the D and Li atoms to be located. The refined structure ($P4/nmm$, $a$ = 3.79756(2), $c$ = 10.30704(8) Å at 5 K) is shown in Figure 3, and the refined parameters are supplied in Tables S3−S6. The refined composition of $Li_{0.6(1)}(ND_{2.7(1)})_{1.7(1)}Fe_2Se_2$ carries large uncertainties due to intrinsic disorder in the material, large displacement ellipsoids, and significant parameter correlations resulting from the limited $Q$-range at high $Q$ available on WISH. The less-than-full nitrogen site occupancy is consistent with the volumetric absorption of ammonia (see below), and a refined D:N ratio <3 is consistent with the ammonia-poor material containing some amide moieties.[8] The Fe−Se distances of 2.415(1) Å and the Se−Fe−Se angles of 103.65(3)° (×2) and 112.46(2)° (×4) are very similar to the values in the ammonia-poor intercalate at 8 K (Se−Fe−Se = 104.40(8)° (×2) and 112.06(4)° (×4); Fe−Se = 2.408(1) Å), consistent with a nonredox intercalation of further ammonia. The ammonia and amide moieties are modeled as orientationally disordered, and there are N−D···Se hydrogen bonds with a D···Se separation of 2.756(4) Å, similar to that in the ammonia-poor intercalates (2.761(3) Å).[8] The freely refined N−D distances of 0.955(4) and 0.884(5) Å, the D···N separation of 2.719(5) Å between adjacent $ND_3$ molecules, and the Li−N distance of 2.1837(6) Å are comparable to the distances found in solid $ND_3$ (N−D = 1.012(2) Å; D···N = 2.357(2) Å at 2 K),[15] $LiND_2$ (Li−N = 2.065(3)−2.210(3) Å, N−D = 0.967(5) and 0.978(6) Å),[16] and $Li(ND_3)_4$ (Li−N = 2.035(5)−2.078(5) Å; N−D mean of 0.99 Å).[17]

The orientation of the ammonia molecules relative to the selenide and lithium ions is qualitatively similar to the arrangement in the hydrated superconducting phase of $Na_{0.3}CoO_2{\cdot}1.2D_2O$ ($T_c$ = 4.5 K), described in detail by Jorgensen et al.[18] That compound also contains a double layer of small polar molecules which in that case separates sodium ions from the transition-metal-containing layers. In both systems there is hydrogen bonding between the hydrogen atoms of the small molecule and the anion of the transition-metal layers, and the hydrogen atoms located toward the center of the intercalate layer avoid the positively charged alkali metal ion.

To probe further the reversible sorption of ammonia by the ammonia-poor Li/ammonia intercalate, an 8 g portion of the $ND_3$-poor intercalate was placed in a steel pressure cell, briefly evacuated, and then placed in a closed-cycle refrigerator on WISH. The sample was cooled to 250 K and, with PND data collected continuously, was exposed first to a constant 1 atm of $ND_3$ and second to a 500 $cm^3$ buffer volume of $ND_3$ initially at 1 atm. In both cases the sample was observed to absorb $ND_3$ extremely rapidly with 90% of the $ND_3$ absorbed from the buffer volume within 45 min, consistent with the refined composition. Between these two charging experiments the sample was exposed to a dynamic vacuum at 260 K and was observed to desorb all the additional $ND_3$, to regenerate the $ND_3$-poor intercalate. The evolution of the neutron diffractograms is shown in Figure 4.

The $NH_3$ absorption isotherm at 260 K was subsequently measured on 1.039 g (3.575 mmol) of $NH_3$-poor Li/$NH_3$ intercalate (Figure 4, top) with an automated gas sorption analyzer (QUANTACHROME Autosorb iQ). The uptake of $NH_3$ of 72.6 $cm^3/g$ corresponds to the adsorption of ∼0.9 mol of $NH_3$ per mole of $Li_{0.6}(NH_{2.8})Fe_2Se_2$[8] at 1 atm (theoretical value: 79.0 $cm^3/g$), supporting the conclusions of the PND measurements that ammonia molecules do not fill all the available crystallographic sites under the synthetic conditions. The isotherm shows rapid adsorption of $NH_3$ once the $NH_3$ pressure reaches 0.2 atm, and the isotherm is hysteretic with appreciable desorption of $NH_3$ at 260 K only occurring when the pressure is reduced to 0.1 atm above the solid. This profile is typical for interlamellar intercalation of polar molecules as described by


dx.doi.org/10.1021/ja411624q | J. Am. Chem. Soc. 2014, 136, 630−633

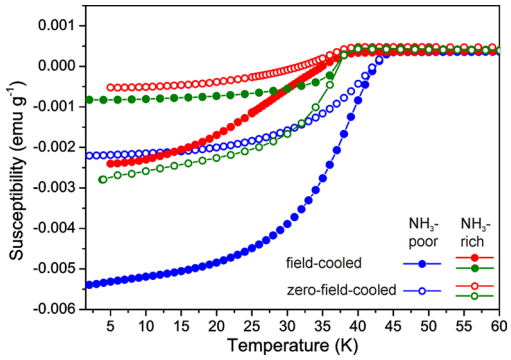


**Figure 5.** Magnetic susceptibilities of an ammonia-rich intercalate (green) suspended frozen in some of the ammonia used in its synthesis (see SI) and an ammonia-rich intercalate (red) synthesized by exposing the ammonia-poor intercalate (blue) to 1 atm of gaseous ammonia at −10 °C.

Barrer.[19] The intercalation and deintercalation of $NH_3$ into sodium montmorillonite[20] are strikingly similar to the adsorption and desorption behavior in our case. This isotherm helps to quantify the tendency of the ammonia-rich intercalates to desorb half of their ammonia and explains why the normal use of a Schlenk line (evacuation of the sample container at ambient temperatures) does not enable these materials to be observed easily.

Magnetometry on a sample of the material synthesized using similar apparatus to that used for the *in situ* PXRD measurements and maintained suspended in liquid or frozen ammonia (see SI) revealed a bulk superconductor with $T_c = 39(1)$ K (Figure 5), ∼5 K lower than for the ammonia-poor intercalates.[7,8] A second sample prepared by exposing the ammonia-poor intercalate to 1 atm of $NH_3$ at −10 °C (replicating closely the synthesis of the sample used in the PND experiment and the adsorption experiment) yielded a similar $T_c$. The superconducting volume fractions are estimated to be 30−40%, comparable to those of the ammonia-poor intercalates.[8]

The behavior of the metal/ammonia intercalates of FeSe is strongly reminiscent of the behavior of the hydrates of $Na_{0.3}CoO_2$.[21,22] The ammonia-rich phase identified here corresponds to the hydrated superconductor $Na_{0.3}CoO_2 \cdot 1.2H_2O$,[18,21] and the ammonia-poor material described previously[8] corresponds to nonsuperconducting $Na_{0.3}CoO_2 \cdot 0.6H_2O$.[22] The cobaltates have hexagonal $CoO_2$ layers composed of edge-linked $CoO_6$ octahedra, while the iron selenides have tetragonal layers composed of edge-linked $FeSe_4$ tetrahedra. In the iron selenide system, ammonia-free $K_{0.3}Fe_2Se_2$ corresponding to $Na_{0.3}CoO_2$ has been reported by Ying et al. prepared by deammoniation at 200 °C,[12] and the composition $M_xFe_2Se_2$ (M = K, Rb; $x$ estimated as 0.3−0.5)[10,11] appears to be a 33 K superconductor which often coexists as a minor phase intergrown with iron-deficient antiferromagnetic Mott−Hubbard insulators with compositions close to $M_{0.8}Fe_{1.6}Se_2$ synthesized at high temperatures.[11] In the case of the ammonia-poor $Li/NH_3$ intercalate of iron selenide, removal of further ammonia is facile but is accompanied by reduction of iron to the element and eventual formation of $Li_2Se$.[8]

The investigations described here not only expand the range of iron-based high-temperature superconductors and promise further molecular intercalates but also underline how rapid data collection from modern diffractometers allows otherwise fleeting phases to be identified, targeted, and characterized.

## ■ ASSOCIATED CONTENT

### Ⓢ Supporting Information

Experimental details and data. This material is available free of charge via the Internet at http://pubs.acs.org.

## ■ AUTHOR INFORMATION

### Corresponding Author

simon.clarke@chem.ox.ac.uk

### Notes

The authors declare no competing financial interest.

## ■ ACKNOWLEDGMENTS

We thank the UK EPSRC for financial support (EP/I017844), the DFG for the award of a Fellowship to S.J.S., the Diamond Light Source (DLS) Ltd for studentship support for S.J.C. (Cassidy) and S.J.M. We thank M. Kibble for preparing the pressure cell at ISIS. We thank DLS Ltd (EE8691) and ISIS for beamtime.

## ■ REFERENCES

(1) Sefat, A. S. *Curr. Opin. Solid State Mater. Sci.* **2013**, *17*, 59.
(2) Johrendt, D. *J. Mater. Chem.* **2011**, *21*, 13726.
(3) Fujitsu, S.; Matsuishi, S.; Hosono, H. *Int. Mater. Rev.* **2012**, *57*, 311.
(4) Hirschfeld, P. J.; Korshunov, M. M.; Mazin, I. I. *Rep. Prog. Phys.* **2011**, *74*, 124508.
(5) Hsu, F.-C.; Luo, J.-Y.; Yeh, K.-W.; Chen, T.-K.; Huang, T.-W.; Wu, P. M.; Lee, Y.-C.; Huang, Y.-L.; Chu, Y.-Y.; Yan, D.-C.; Wu, M.-K. *Proc. Natl. Acad. Sci. U.S.A.* **2008**, *105*, 14262.
(6) McQueen, T. M.; Huang, Q.; Ksenofontov, V.; Felser, C.; Xu, Q.; Zandbergen, H.; Hor, Y. S.; Allred, J.; Williams, A. J.; Qu, Q.; Checkelsky, J.; Ong, N. P.; Cava, R. J. *Phys. Rev. B: Condens. Mater. Phys.* **2009**, *79*, 014522.
(7) Ying, T. P.; Chen, X. L.; Wang, G.; Jin, S. F.; Zhou, T. T.; Lai, X. F.; Zhang, H.; Wang, W. Y. *Sci. Rep.* **2012**, *2*, 426.
(8) Burrard-Lucas, M.; Free, D. G.; Sedlmaier, S. J.; Wright, J. D.; Cassidy, S. J.; Hara, Y.; Corkett, A. J.; Lancaster, T.; Baker, P. J.; Blundell, S. J.; Clarke, S. J. *Nat. Mater.* **2013**, *12*, 15.
(9) Scheidt, E.-W.; Hathawar, V. R.; Schmitz, D.; Dunbar, A.; Scherer, W.; Mayr, F.; Tsurkan, V.; Deisenhofer, J.; Loidl, A. *Eur. Phys. J. B* **2012**, *85*, 279.
(10) Texier, Y.; Deisenhofer, J.; Tsurkan, V.; Loidl, A.; Inosov, D. S.; Friemel, G.; Bobroff, J. *Phys. Rev. Lett.* **2012**, *108*, 237002.
(11) Shoemaker, D. P.; Chung, D. Y.; Claus, H.; Francisco, M. C.; Avci, S.; Llobet, A.; Kanatzidis, M. G. *Phys. Rev. B: Condens. Mater. Phys.* **2012**, *86*, 184511.
(12) Ying, T.; Chen, X.; Wang, G.; Jin, S.; Lai, X.; Zhou, T.; Zhang, H.; Shen, S.; Wang, W. *J. Am. Chem. Soc.* **2013**, *135*, 2951.
(13) Williams, G. R.; O'Hare, D. *Chem. Mater.* **2005**, *17*, 2632.
(14) Coelho, A. A. TOPAS Academic: General Profile and Structure Analysis Software for Powder Diffraction Data, 5th ed.; Bruker AXS: Karlsruhe, Germany, 2012.
(15) Hewat, A. W.; Riekel, C. *Acta Crystallogr. A* **1979**, *35*, 569.
(16) Sørby, M. H.; Nakamura, Y.; Brinks, H. W.; Ichikawa, T.; Hino, S.; Fujii, H.; Hauback, B. C. *J. Alloys Compd.* **2007**, *428*, 297.
(17) Ibberson, R. M.; Fowkes, A. J.; Rosseinsky, M. J.; David, W. I. F.; Edwards, P. P. *Angew. Chem., Int. Ed.* **2009**, *48*, 1435.
(18) Jorgensen, J. D.; Avdeev, M.; Hinks, D. G.; Burley, J. C.; Short, S. *Phys. Rev. B: Condens. Mater. Phys.* **2003**, *68*, 214517.
(19) Barrer, R. M. *Pure Appl. Chem.* **1989**, *61*, 1903.
(20) Barrer, R. M.; MacLeod, D. M. *Trans. Faraday Soc.* **1954**, *50*, 980.
(21) Takada, K.; Sakurai, H.; Takayama-Muromachi, E.; Izumi, F.; Dilanian, R. A.; Sasaki, T. *Nature* **2003**, *422*, 53.
(22) Takada, K.; Sakurai, H.; Takayama-Muromachi, E.; Izumi, F.; Dilanian, R. A.; Sasaki, T. *J. Solid State Chem.* **2004**, *177*, 372.